

A COUPLED CFD FINITE ELEMENT ANALYSIS METHODOLOGY IN A BIFURCATION PIPE IN A NUCLEAR PLANT HEAT EXCHANGER

J. A. Dixon, A. Guijarro Valencia, P. Ireland, P. Ridland
Rolls-Royce plc, UK

N. Hills
University of Surrey, Guilford, UK

Abstract

The accurate calculation of temperature distribution in key parts of a nuclear plant plays a crucial role in maximising the power output and the plant efficiency, whilst ensuring safe operation. The need for making the most profitable use of the available sources of energy requires the full exploitation of plant operational capacity. Temperature dependent material properties mean that increasing the power output in a nuclear plant may reduce the life of the welds in the pipes of the heat exchanger (boiler), operating in very demanding conditions. Rolls-Royce plc was requested to come up with a suitable solution that shielded critical pipe weld locations, reducing local temperatures, so allowing a useful increase in power output from the plant. Part of the heat shield design process was a comprehensive thermal analysis of the installation. Traditionally fluid and solid simulations are conducted separately or using conjugate analysis. Standard methods rely on the application of boundary conditions to the wall surface, which are commonly based on empirical heat transfer coefficient correlations or approximate read across of the CFD results. An alternative approach using conjugate calculations can be adopted, but the computational cost and meshing difficulties in matching the fluid and solid grids makes this unaffordable in terms of analysis time. This paper presents the application of an improved method using a communication library (SC89) between the in-house finite element (FE) code SC03, and the commercial computational fluid dynamics (CFD) code FLUENT. The method has been validated using test data from a Perspex model, where heat transfer coefficients were measured using a transient liquid crystal technique.

Nomenclature

D	Diameter	(m)
h	Heat transfer coefficient	(W/m ² K)
k	Thermal conductivity	(W/m K)
L _c	Characteristic length	(m)
\dot{m}	Mass flow rate	(kg/s)
q	Heat flux	(W/m ²)
T	Temperature	(K)
t	Time	(s)
U	Velocity	(m/s)
Re _t	Steam Re Number	

Re _{re}	CO ₂ Re Number	
ΔT	Temperature difference	(K)
δ	Non dimensional diameter	
θ	Non dimensional temperature	
μ	Dynamic viscosity	(kg/m s)
ρ	Density	(kg/m ³)

Subscripts

f	Fluid
m	Metal
w	Wall

1. INTRODUCTION

Rolls-Royce plc was awarded a contract from a power generation customer to design heat shields for two critical regions of the boiler (heat exchanger) assembly of a civil nuclear reactor plant. In order to support the design of these heat shields a thermal analysis of the local installation is required, i.e. to determine the local pipe work temperature reductions made possible by the heat shields. It is understood that the plant is currently restricted to operating at a certain power capacity (nominal), due to boiler pipe weld temperature level restrictions. For reasons of improving the plant efficiency it is desirable to run the plant at a higher power condition (design); a 20 % increase has been suggested as a suitable target. Two locations were identified as critical, i.e. the bifurcation pipe and tailpipe welds. A shroud for each component of the boiler was designed at Rolls-Royce plc under the task leadership of the Civil Nuclear Division. The Thermals Team in Rolls-Royce plc Gas Turbine Supply Engineering was engaged to conduct the thermo-mechanical analysis of these designs. This paper presents the results of the bifurcation pipe analysis and the experimental verification carried out in a Perspex test rig. The novelty of this work is on the application of a

coupled CFD-FEA solution in a heat exchanger with an internal (superheated steam) and an external fluid (CO₂ gas).

In the initial phase, a 3D thermal model was created and run using traditional stand-alone FEA based on heat transfer coefficient empirical correlations, using the proprietary software SC03 [4].

In a second stage of the analysis, CFD FLUENT models were created in order to get more accurate predictions of h , focusing in the main weld, located at the bifurcation mid height. The calculation was initially run adiabatically. Afterwards, temperature profiles read from the CFD were applied and, from the new solution, heat transfer coefficients were extracted to read across to the SC03 model as explained by Alizadeh et al. [3]. At this stage, the experimental data from the Perspex test rig was available and allowed validation of the h calculated from the CFD. Very good agreement between the measurements and the numerical solution was observed.

The final step was to couple the FE SC03 model with the CFD results using the plugin (communication library) SC89. The methodology and the models are described in Section 5 below.

In parallel to the computational analysis, a test rig was run. The tests were performed in the Heat Transfer Facility at Rolls-Royce plc Bristol. The conventional transient, liquid crystal experiment used by Rolls-Royce plc Turbine Systems was adapted for this application. The model scale is the same as the power station and is operated at equivalent Reynolds number conditions. A brief description of the experiment and the results for verifying the stand alone CFD are included in this paper.

1.1 Geometry and materials.

The geometry of the analysis can be seen in Figure 1. It was provided by the customer and recreated in CAD format by the Rolls-Royce plc NNPI design team. The bifurcation consists of two pipes that combine into one that collects and mixes the steam from individual pipes in the boiler (heat exchanger). Physically, the assembly consists of four parts: two elbow pipes of different through flow diameter and bend radii; a sawn bend tube and a connection tube that merges the pipes as described previously. The parts are welded together and connected to longer pipes in the boiler. The critical section of the installation is the main weld that connects the sawn tube with the nozzle. In the heat shield design improvement proposal the welds were required to be insulated as much as possible from the hot gas.

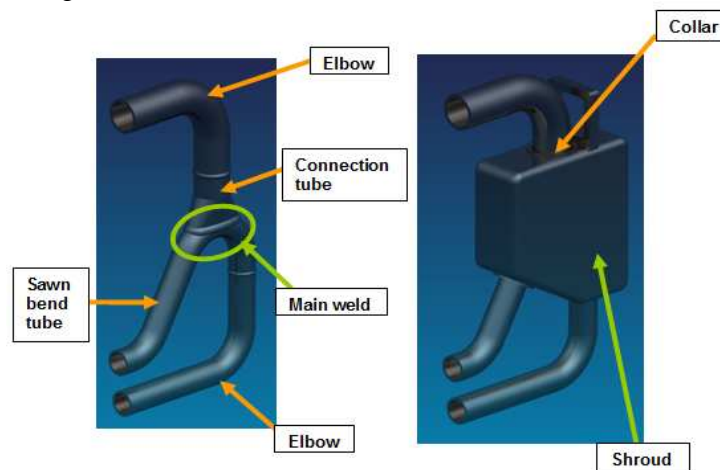


Figure 1 – Extent of the geometries in the analysis. 1a, Left, un-shrouded bifurcation, 1b right shrouded pipes.

The heat shield designed was a stainless steel shroud. The installation consists of two metallic shells that enclose the pipe work. At the interface with each tube, a metallic collar was placed to minimize the possible leakage of hot CO₂ into the shroud. The design team worked out the maximum clearance between the bifurcation pipes and the collars of the shroud. Figure 1 b shows the geometry used in the analysis i.e. the bifurcation with the shroud in place.

The dimensions of the pipes are given as a fraction of a characteristic dimension, L_c , equal to the distance between the bottom and the top of the bifurcation. Hence, the bottom tube internal diameter is of $\delta=0.0628$ whereas the top elbow pipe diameter of the bifurcation is of $\delta=0.0854$.

1.2 Operating conditions.

The installation operates in a nuclear power plant at nominal power output capacity, although the desired working conditions for the installation is at a 20 % higher output (namely design conditions). Table 1 shows the environmental variables in which the bifurcation works. The values have been made non-dimensional based on the CO₂ thermodynamic properties at the design condition, except the steam mass flow rate, non-dimensionalized based on the design point. In addition, the flow Re number for each fluid has been included in the table as defined in the nomenclature section. For the steam, Re_t is defined as a function of the outlet pipe radii whereas for the reactor gas Re_{re} , L_c is the same as for the geometry definition from the previous section.

Reactor Power	Nominal conditions	Design Conditions	Δ (%)
Reactor Gas Temperature	0.963	1	3.84
Reactor Gas Pressure	1	1	0
Reactor Gas Velocity	0.985	1	1.52
Reactor Gas Density	1.019	1	-1.86
Re_{re}	$1.68 \cdot 10^6$	$1.68 \cdot 10^6$	---
Steam Temperature	0.608	0.635	4.49
Steam Pressure	3.252	3.625	11.48
Steam Mass Flow Rate	0.888	1	12.61
Re_t	10300 (10352)	11693 (11700)	---

Table 1 – Nominal and design conditions in the installation.

The table shows that the bifurcation will be exposed with the new operating conditions to an overall temperature raise of about 4%. In this condition, the customer requirement was that the temperature reduction in the external weld surface must be more than $\theta=0.0185$.

2. MODELS AND ASSUMPTIONS

The work presented is based on the analysis carried out with an in-house software tool, SC03, and a commercial code, FLUENT. SC03 is a finite element code performing transient thermal and mechanical analysis. For this paper, the comments will be focused in the application for the thermal problem. Although the numerical method implemented is common to many of the commercial solvers available, it is specifically designed for turbomachinery applications due to a wide range of specialist thermal modelling features. A description of the SC03 code and its use in engine thermal analysis is given by Armstrong et al. [4].

2.1 FE Models.

The fully 3D models were meshed using 10 node tetrahedrons. The resulting finite element meshes consisted of 66421 nodes, 33176 elements in a single domain for the bifurcation model and 97380 nodes, 48690 elements in 2 domains for the model with the shroud in place.

The material properties for the SC03 model were read from the Rolls-Royce plc Material Properties (COMMIT) Database. The fluids passing through and surrounding the relevant feature are superheated steam (inside) and CO₂ (outside). The fluid properties for these materials are not available in the SC03 libraries; hence these had to be imported from external sources. Two SC03 data files were created in the appropriate format to be readable by the code, as defined in the Rolls-Royce plc Thermo-mechanical Analysis best practices. The steam properties were extracted from the latest water and steam properties, using the tables released by the International Association for the Properties of Water and Steam [6], whereas the CO₂ properties were extracted from the Fluent database [5].

The model was run to a steady state point at the conditions referred to above. This was achieved using a transient cycle consisting of a 10 second ramp from the initial condition, and a ‘flat’ steady condition of 2000 seconds.

2.2 Thermal boundary conditions.

In SC03 convective and radiative heat transfer boundary conditions are applied to the pipe surfaces in contact with the fluids.

For the un-shrouded bifurcation, the model is divided into two zones (Figure 2a):

- Inside: SC03 'stream' (finite source advection), boundary conditions were applied. For the circular pipes, the Nunner heat transfer coefficient [9] correlation was used. At the bifurcation, where the flow mixes, the average of the large and small pipe calculated htc's was used, as both pipe htc's were very similar.
- Outside, two boundary conditions were considered:
 - An SC03 convecting zone, ('infinite' heat source) was applied in the model, with the CO₂ temperature applied and a htc calculated with the Sieder-Tate correlation [10], assuming a square pipe surrounding the bifurcation of a certain cross sectional area consistent with the CFD model and the plant geometry.
 - External radiation. The remote temperature was taken as the CO₂ temperature and the emissivity 0.8 (read from tables for polished stainless steel). This corresponded to the worst possible scenario of radiation to the pipes.

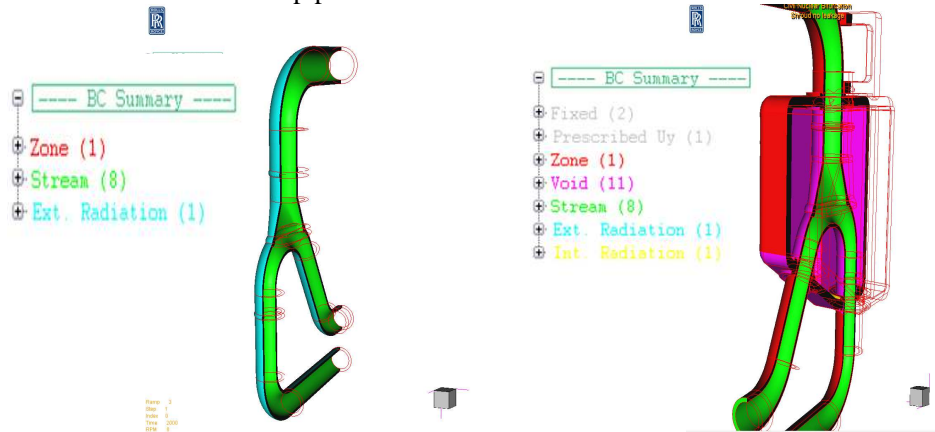


Figure 2 Un-shrouded 2a) and shrouded 2b) bifurcation boundary conditions.

- For the shrouded bifurcation, three zones were defined instead (Figure 2b).
- For the steam pipe internal surfaces, the boundary conditions were kept the same as for un-shrouded installation.
- Outside the shroud and at the external faces of the bifurcation, an infinite source (SC03 convecting zone) was applied, as for the un-shrouded bifurcation model. The heat transfer coefficient (htc) correlation was assumed to be the same as for the un-shrouded model but modified to account for the new cross sectional flow area. Also, specifying external radiation with an emissivity value of 0.8, and a remote temperature of the hot gas temperature. A different boundary condition was applied at the lower surface of the shroud. There, the flow was assumed to separate and, thus, the correlation for natural convection below a horizontal inverted flat plate was applied [2]. At the collars, the leakage was modelled with a heat finite source (SC03 stream). Initially, the mass flows were worked out based on a hand calculation: $m=0.377\%$ of the steam mass flow rate. Later on this value was refined, based on the CFD results.
- Inside the shroud box, a controlled volume heat balance (SC03 void) was applied with the corresponding natural convection correlation for each of the surfaces. The void was also vented by the leakage at the gap. In addition to this, internal radiation was applied.

2.3 CFD model.

Three CFD models were created to model the fluid conditions in the different areas of the bifurcation. Common to all of them was the software to create the meshes, ICEM CFD v11, and the topology, unstructured (based on tetrahedral cells) with layers of prismatic cells close to the solid walls. The worst tetrahedral quality (cell aspect ratio) was fixed to be 0.1. This was achieved in the steam and un-shrouded CO₂ models. For the shrouded models, the worst quality value was not as

good, 0.01, in some cells close to the collar leakage gap. This region was monitored using a static temperature point probe in every moment showing no divergence issues.

Regarding the FLUENT v6.3.26 set up, the k-epsilon turbulence model with enhanced wall functions was used for the analysis, see section 12.10.4 in the Fluent User Guide [5]. Following these guidelines, the grids were created to get y^+ values lower than 10 and ~ 1 in the proximity of the weld. The fluids were modelled as incompressible-ideal gas, as the flow Mach number was below 0.1 at all points in the fluid domain. The segregated solver in double precision mode was chosen. The equations were run initially in first order and after a number of iterations were switched to second order.

The calculations were performed on a Xeon 8 core 2 GHz processor 64 bit Windows Vista machine. Full convergence was reached in about 20000 iterations for all of the models in about 80 hours.

2.3.1 Steam CFD model.

The computational domain was the interior volume of the pipe. The mesh is unstructured, and a prismatic layer of 12 cells 'depth' was applied all around the walls, with a first cell size of 0.001 mm and an expansion ratio of 1.2. The grid consisted of 2356810 cells and 802674 nodes.

The boundary conditions in the model were defined as follows:

- Two **inlets** are defined in the model. Both were defined as mass flow inlet with specified inlet total temperature as for the design conditions. The turbulence intensity was $TI=5\%$ hydraulic diameter equal to the pipe inlets.
- The **walls** were defined as viscous and adiabatic, firstly, and isothermal later on. The applied temperature was extracted from the SC03 model, area averaged at the weld, uniform at the walls.
- The **outlet** was defined as a pressure outlet, with a gauge pressure $p=0$ Pa.

2.3.2 Un-shrouded CO₂ CFD model.

For this model, the computational domain was defined as a box around the pipe of twice L_c in the longitudinal pipe dimension and a length of $0.5 L_c$ in the horizontal direction. This was specified to ensure linear periodicity between different pipes. The grid consists of 2996146 cells and 610024 nodes with a prismatic layer of 10 cells 'depth' and a first cell size of 0.01 mm and an expansion ratio of 1.2.

The boundary conditions in the CFD model are:

- The **inlet** was modelled as velocity inlet normal to the boundary as for the design condition. The turbulence intensity was $TI=1\%$ and the hydraulic diameter corresponding to the box inlet.
- The **walls** were defined as viscous and, equally, adiabatic first and then isothermal. The applied temperature was extracted from the SC03 model.
- The **outlet** was defined as pressure outlet with a gauge pressure $p=0$ Pa.
- The **surrounding boundaries**, namely front, back and periodic, were defined as symmetry boundary conditions, modelling the free stream conditions around the weld.

2.3.3 Shrouded CO₂ CFD model.

The same extent of the domain was used as in the previous case. The cell and node count is now 3375059 cells and 1117183 nodes. At the bifurcation, 6 cells have been applied all around the walls, with a first cell size of 0.01 mm and an expansion ratio of 1.2. At the shroud, three layers were applied.

At the collars, the near wall cell size was 0.003 mm, to be able to apply up to 6 cells in the bifurcation side and 3 in the collar side.

The boundary conditions remain unchanged from the previous model.

3. PERSPEX TEST RIG DESCRIPTION

The heat transfer coefficient over the surface of the bifurcation was measured using the transient heat transfer method developed for evaluating turbine blade cooling systems- see Ireland Jones [7]. The technique subjects an insulated model to a change in gas temperature and measures the model surface temperature with a coating of temperature sensitive liquid crystals. The bifurcation was

tested over a range of Reynolds number in a rectangular wind tunnel, Figure 3, with a cross-section designed to achieve conditions representative of the periodically spaced bifurcations in the power station. The dimensions allowed for boundary layer displacement thickness growth on the two tunnel side walls. The wind-tunnel is fed from the laboratory compressed air supply through a choked orifice installed upstream of a cylindrical, perforated flow distributor. The tunnel is divided into two parts. The upstream section includes the flow distributor, pressure drop flow resistance (a sheet of Scotchbrite) and honeycomb flow straightener (not shown). A heater mesh is installed between the flanges that join the two sections. The fast response heater mesh consists of two sheets of fine stainless steel mesh that produce a step change in temperature. A bursting disc is connected to the upstream section. The bifurcation is installed in the larger section. The flow exhausts through two 100mm diameter hoses to the lab vacuum system.

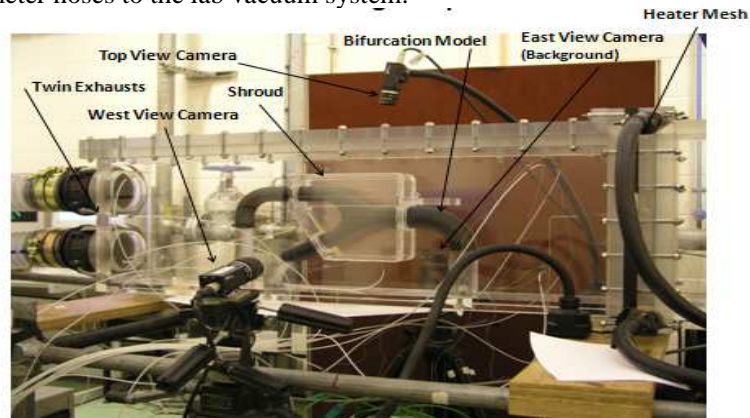


Figure 3 - Photograph of the rig set-up, with the main features highlighted. Flow is from right to left.

The air temperature is increased by the Heater Mesh to give a test gas temperature of about 60°C. The regions of interest on the model were painted with black paint and then coated with a thermochromic liquid crystal. The crystal undergoes a colour change at a specific, calibrated temperature (either 35°C or 30°C), which is recorded by video cameras. The change time at each pixel is related to the driving gas temperature and a htc value is calculated for each pixel.

The h results are scaled to power station conditions using standard methods developed for turbine blades and other Rolls-Royce heat transfer research. These are well summarised in the case of fire simulation by Abu Talib et al. [1]. In broad terms, two main parameters affect the scaling of h, specifically the Reynolds number and gas thermal conductivity. The htc levels measured were then converted to power station conditions using dimensional similitude. The scaling factor at 100% flow is **1.82**.

4. STAND-ALONE SOLUTION AND TEST DATA VERIFICATION

In this section, some representative results will be described. Although the main objective is to show the stand-alone solution to allow benchmarking with the coupled analysis results, the effect of the shroud in the installation will be also assessed. In addition to this, the results of the test rig and the comparison done with the stand-alone CFD is shown. All the temperature values are shown in non-dimensional form based on the CO₂ inlet total temperature. The htc values are defined as

$$htc = q / (T_w - T_f) \quad (1)$$

where T_f is:

- The boiler gas temperature for the bifurcation un-shrouded.
- The CO₂ temperature inside the enclosure either calculated in the CFD or measured in the tests.
- The steam inlet temperature inside the pipes.

4.1 SC03 predictions based on correlations.

Figure 4a shows metal temperature predictions for the bifurcation pipe at the design point. The maximum temperature is around $\theta=0.899$ at the upper weld. The area averaged metal temperature at the main weld is $\theta=0.898$. Figure 4b shows metal temperature predictions at the bifurcation with the

shroud in place. The area averaged face wall temperature is $\theta=0.880$. The solution shows some of the limitations of the traditional modelling. Although the heat transfer coefficients were chosen to model correctly the external temperature at the welds, on the pipes the contours look uniform showing none of the actual fluid behaviour, as will be shown later in this paper.

This initial result met the customer requirement, as the reduction in temperature is $\theta=0.018$ for the worst case scenario.

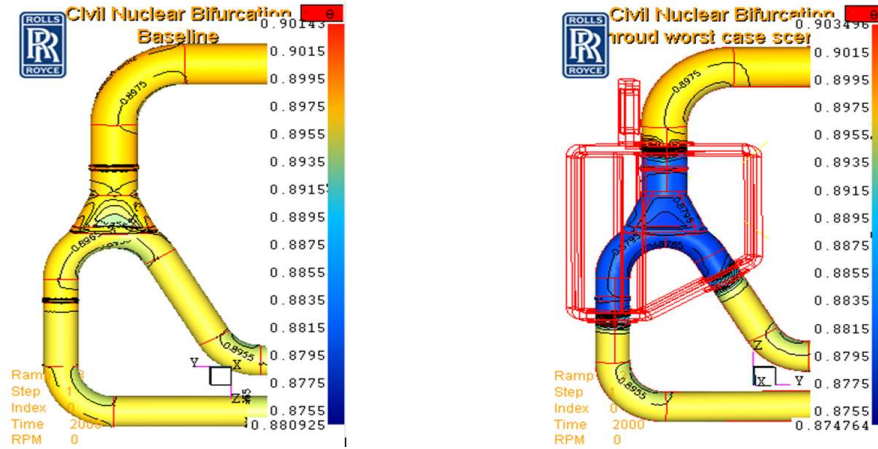


Figure 4 – Contours of metal temperature at the bifurcation outer face un-shrouded (4a) and shrouded without showing the heat shield (4b). Stand alone SC03 solution.

4.2 CFD stand alone solution and comparison with test data.

The CFD was used to extract heat fluxes, fluid temperatures and mass flows through the collar. In this section the focus will be on the flow patterns and their implications in terms of heat transfer coefficient.

Figure 5a shows streamlines coloured by velocity magnitude. The flow is, as expected, unsteady in many parts of the fluid field i.e. downstream in the tubes where the CO₂ is showing the typical von Karman vortices street for laminar flows. However, close to the weld, the fluid behaves steadily and is sufficiently far away from the horizontal pipes wake.

Figure 5b shows streamlines inside the box coloured by velocity magnitude. The picture justifies the use of a void boundary condition with natural convection, as applied in the SC03 model. The flow velocities in all the control volume are under 1 m/s and the mean average value is around 0.2. This means that the Re number, based on the size of the box is of the order of 10⁴. In addition to this, the flow structure is highly chaotic and a number of vortices flowing in all the space directions are shown, making it extremely complicated to assign a flow direction to the thermal model. This will also cause the htc coefficients not to be symmetric in the model, although the variation in time will be small (see below).

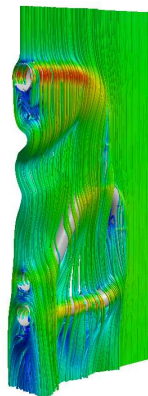


Figure 5a) – Streamlines at the un-shrouded bifurcation coloured by velocity magnitude.

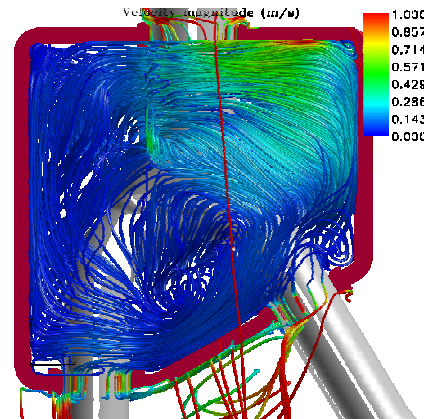


Figure 5b) – Streamlines at the shrouded pipes inside the heat shield.

These results were benchmarked with the results from the test rig. Figure 6 compares the weld htc for the un-shrouded case. In general, the CFD appears to be slightly lower than the experiments but the agreement is generally within 10%. The CFD under-predicts the level on the centre line (CL) by about 15%. This means that the benefit in pipe temperature achieved by fitting the shroud may be under-estimated. Nevertheless, there is a narrow region of significant discrepancy in the trough behind the weld. The CFD predicts a higher htc level than measured. This is most likely a region of separation, which is challenging to model with CFD. Fortunately this region is narrow and will not significantly affect the thermal model.

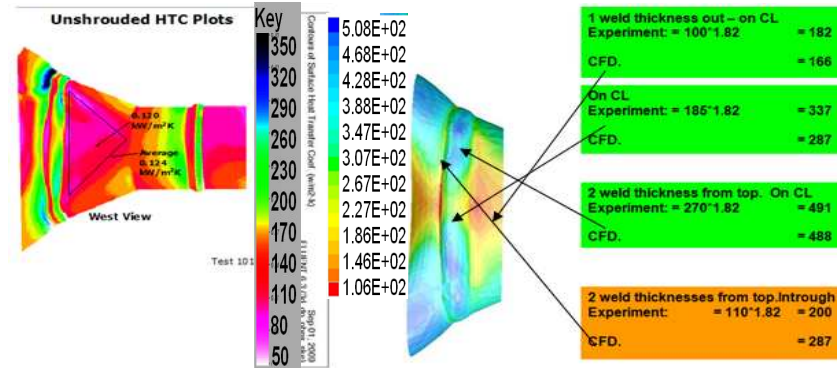


Figure 6 - htc plots of un-shrouded tests at 100% condition analysed using gas stream temperature.

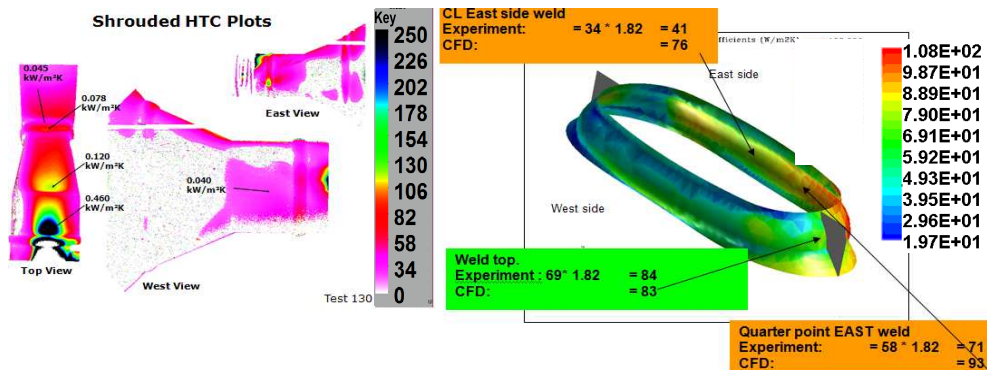


Figure 7 - htc plots of shrouded tests at 100% condition analysed using gas stream temperature.

Figure 7 compares the weld htc for the shrouded case. Both the CFD and experiments show that the shroud has resulted in an asymmetric distribution, and both have the same sense of a-symmetry caused by the vortex shedding. The CFD over-predicts the h by about 22% in the central region of the weld on the EAST side and thus the CFD is conservative. At the top of the weld, the CFD under-predicts the htc. These results, however, may vary slightly in time due to the unsteady nature of the flow. The main conclusion, though, is that the CFD is capturing the values in the correct ‘ball park’, and hence the solution is reliable for predicting the temperature distribution inside the shroud.

The shape of the CFD and the model htc distributions are sensibly consistent. The weld presents itself as a protuberance to the flow and, similar to a turbulator in a turbine cooling passage, corresponds to a zone of elevated htc.

The effect of these discrepancies in h was assessed using a simple 1D model and compared to the stand-alone SC03 predictions. This assessment indicated that the original SC03 model underestimates the benefit of the shroud by approximately a 1.6°C of the desired temperature reduction.

5. COUPLING

5.1 Coupling methodology.

The work presented here is based on the coupling between an in-house software tool, SC03, and a commercial code, FLUENT. A brief summary of the method is given below, while a more detailed description is given by Verdicchio et al. [12].

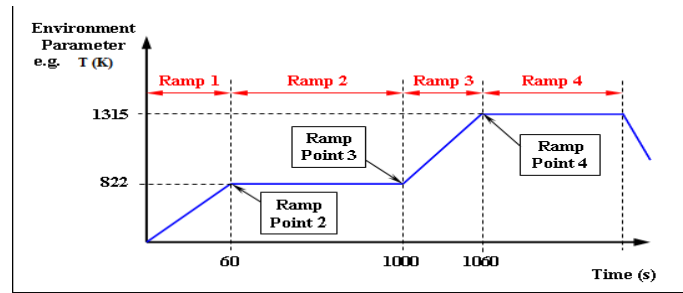


Figure 8 - Cycle definition example

Within SC03, the user defines a transient analysis by specifying an analysis cycle for the particular geometry under investigation, i.e. the evolution of a set of environment parameters through the time span simulated. These are user-input parameters and include mass flow rates, operating temperatures and pressures (a typical example is given in Figure 8). The code is time marching and as such, SC03 needs an initial condition i.e. an initial metal temperature distribution for each node in the solid. To solve the heat equation in the solid, SC03 uses an implicit time discretisation and a Newton-Raphson solver [4].

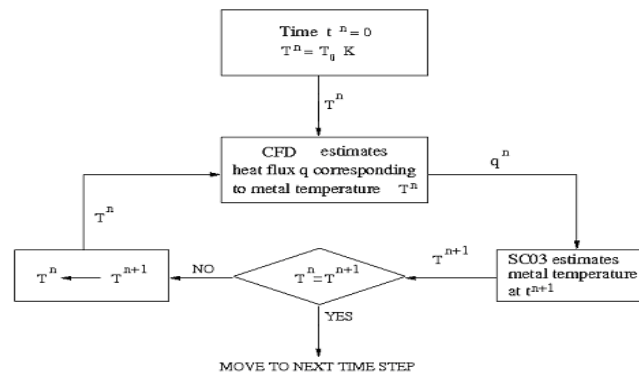


Figure 9. Schematic representation of the coupling process.

The thermo-mechanical coupling process is schematically depicted in Figure 9. First, the system invokes the fluid solver FLUENT, passing to it the current values of boundary temperatures T^n (the superscript n indicates that these quantities refer to the temporal level t^n). An important assumption is made here: as the fluid response to a change of operating conditions occurs on time scales much shorter than that appropriate to the metal heat conduction, the influence of unsteadiness in the fluid is expected to be negligible, and steady CFD calculations can be employed using the boundary conditions passed by SC03 [8,11]. More precisely, the CFD solver applies the wall temperature boundary conditions passed from SC03 and runs a steady state case to find the solution corresponding to these prescribed wall temperatures. After a certain degree of convergence has been achieved, based on user inputs, FLUENT outputs the heat fluxes q^n computed on the boundaries. These heat flux values are returned to SC03, which runs the Newton-Raphson solver to obtain an improved estimate of the temperature field at time t^n . The CFD solver and the FEA Newton-Raphson solver loop is then repeated until the solution has stabilised to within a user defined tolerance.

When the temperatures are stabilised (typically this requires around five iterations) the analysis moves to the next time step in the analysis cycle. The coupling communications are controlled by the plugin (SC89) of the SC03 program. It is within SC89 that the user specifies one or more coupled walls, outlining a CFD domain, which may cover part or the whole of the finite element model.

5.2 Coupling models set up.

The external and internal radiation boundary conditions remain unchanged from the previous models. However, all the convective boundary conditions were deleted and replaced by coupled

boundary conditions (one per CFD boundary wall), that exchange the heat fluxes and wall temperatures with Fluent, as described in the previous section. The initial domain temperature, T^n at time $t=0$, was assigned to be the steam temperature to help with convergence.

Except at the walls, the CFD boundary conditions are not changed from the previous models. While the option exists within SC89 to use temperatures and mass flows from the FE model at the CFD inlets, in this case, for model stability, the inlet temperature was kept constant during the cycle.

At this stage there is just one additional parameter to set up, which is the number of iterations per CFD call, i.e. the convergence level in the CFD, before passing the information to the FEA model. The maximum number of iterations was set to 100 for every CFD call. A sensitivity study was carried out, running the models to a certain convergence criteria until the maximum change in temperature between solutions was less than 0.1K. This number was reached only in the “power increase ramp”, as during the flat part of the cycle, a convergence criterion based on the energy equation residual, just some few CFD iterations to be run, saving a considerable amount of computational time. One further approximation was made. The models were run with the energy equation only, meaning that the fluid is ‘frozen’, assuming that the flow patterns do not change due to the heat transfer, also that the metal response is much slower than the fluid.

The calculations were conducted on an 8 processor 64 bit Windows Vista machine. The running time was about 17 hours for the un-shrouded model and 26 for the shielded pipe work.

5.3 Coupling results.

In this section, the power of the coupling is shown. The heat flux distribution calculated by Fluent is applied to SC03 identically at the end of the process and these results in a very realistic temperature distribution, shown at the end of this section.

5.3.1 Un-shrouded bifurcation

Figure 12a, the first final result, shows contours of metal temperature at the external surface of the bifurcation. The influence of both fluids can be seen in the picture by benchmarking with the heat flux contours extracted from the CFD (Figure 10a and Figure 10b). The blue contours in the steam domain are areas where the fluid is absorbing heat, and that line up with the red contours in the CO₂ domain, mirroring the behaviour of the steam inside (e.g. the flow separation at the mixing area). However, in the areas of high unsteadiness such as in those affected by the Von Karman street vortices (as seen in Figure 5a), this temperature is expected to be more uniform. This is a limitation in the model (frozen fluid) that must be considered even if it does not affect the main result: the predicted surface average metal temperature in the main weld, at the mid size of the cavity where the fluid behaves steadily, is $\theta=0.897$. In spite of this clear unsteadiness, this only results in a slight asymmetry in the metal temperature distribution, as shown in the previous section.

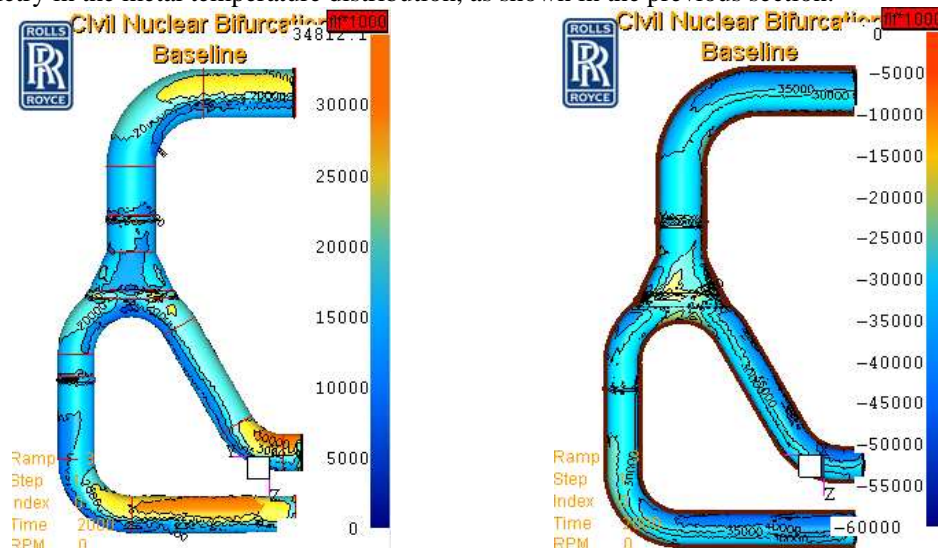


Figure 10 – Contours of heat flux at the un-shrouded bifurcation. The left picture 10a shows the external face surrounded by the gas whilst the right picture 10b shows the internal surface.

5.3.2 Shrouded bifurcation

Figure 11 shows contours of heat flux outside the tubes for both Fluent and SC03. The contours match up very well. The effect of the heat shield is clearly shown in the pictures: the calculated hot side flow is reduced to a minimum ($m=0.2\%$ of leakage though the collar), and hence, the level of heat transfer to the metal is also reduced. Note that this leakage is calculated by the CFD analysis, and applied in the coupled analysis without any estimated or measured leakage flow at the shroud collar position.

Figure 12b shows contours of surface metal temperature for the shielded bifurcation. As in the unshrouded model, the distribution is now more realistic. The flow is still unsteady although two comments can be made here: outside the shroud, the hardware breaks the shedding and that reduces the unsteady behaviour in the CO_2 ; inside, the flow is totally unsteady, although as the heat fluxes in the fluid are driven by conduction the solution is clearly acceptable.

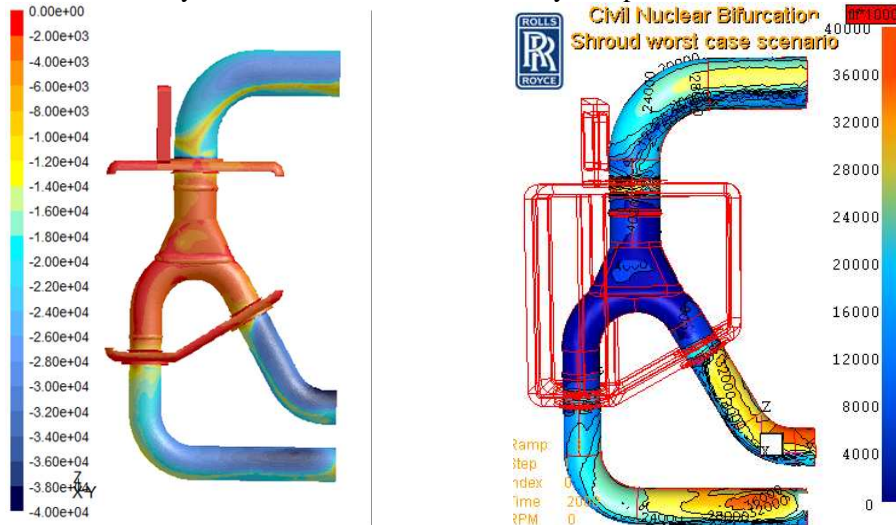


Figure 11 – Contours of heat flux at the shrouded bifurcation inside the box. The left picture 11b shows the Fluent solution whilst the right picture 11b shows the SC03 contours applied by SC89.

From these metal temperature contours, the area averaged surface metal temperature in the weld has been extracted, being equal to $\theta=0.880$. The figures below are the final solution.

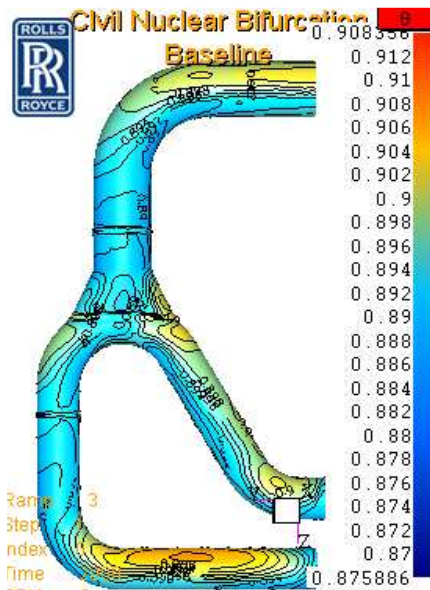


Figure 12a - Contours of metal temperature at the un-shrouded bifurcation. Coupled solution

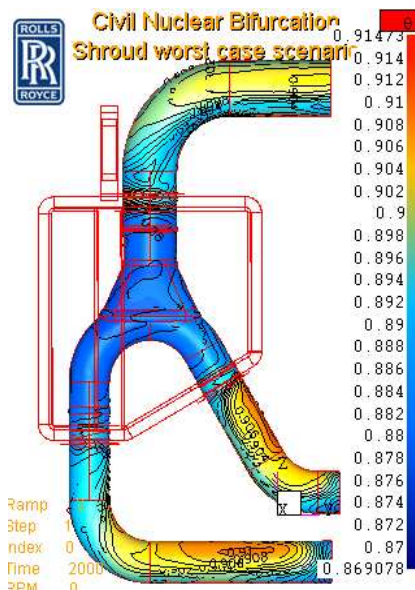


Figure 12b -Contours of metal temperature at the shrouded bifurcation. Coupled solution

Conclusions

The main conclusion is that the mechanics of the Rolls-Royce plc CFD/FE coupling method has been successfully run for the very first time in a heat exchanger configuration with two different fluids. The model is robust, runs quickly and produces a reliable solution capturing features that the stand-alone models can not predict.

The method produces a very similar answer to the traditional stand-alone calculation, which is really encouraging, i.e. leading to the expectation of producing more accurate heat transfer models in the future, when CFD analysis is applied in conjunction with the FE conduction analysis. The running time compared to the 'read-across' method time, i.e. from a CFD solution to an SC03 standard model, is comparable or smaller, and has the potential of capturing the recirculations and flow behaviour correctly, also minimizing the number of user specified boundary conditions applied to the models.

Acknowledgments

The authors want to acknowledge the customer for selecting Rolls-Royce plc for this project, also the Rolls-Royce plc Civil Nuclear Team for having the confidence to engage the gas turbine Thermals team to carry out this analysis. Thanks also to the project members Lionel Reyes, Mark Goodson and Shoja Farr for their contribution. Finally, a special mention must be made to Christopher Barnes for his technical support and advice using SC89.

References

- [1] Abu Talib, A-R, Neely, A.J., Ireland, P.T., Mullender, A.J., (2005) "Comparison between heat flux measurements made on the standard fire-certification propane-air burner with levels derived from the low temperature analogue," *Journal of Engineering for Gas Turbines and Power*, Vol. 127, Issue 4.
- [2] W H McAdams, *Heat Transmission*, Third Edition, McGraw-Hill, 1958
- [3] Alizadeh, S., Saunders, K., Lewis, L.V. and Provins, J. "The Use of CFD to Generate Heat Transfer Boundary Conditions for a Rotor-Stator Cavity in a Compressor Drum Thermal Model", *ASME paper GT2007-28333*. (2007)
- [4] Armstrong, I. and Edmunds. T.M. "Fully Automatic Analysis in the Industrial Environment", *Proceedings of 2nd International Conference on Quality Assurance and Standards, NAFEMS*. (1989)
- [5] FLUENT Inc. Lebanon, New Hampshire. User Guide for version 6.3 (2006)
- [6] IAWSP Release on the IAPWS Formulation 2008 for the Viscosity of Ordinary Water Substance. (2008)
- [7] Ireland, P. T. and Jones, T.V. "Liquid crystal measurements of heat transfer and surface shear stress", *Measurement Science and Technology*, vol. 11, Number 7, July 2000 *Institute of Physics*. (2000)
- [8] Illingworth, J.B., Hills, N. J. and Barnes, C.J.. "3D Fluid-Solid Heat Transfer Coupling of an Aero Engine Pre-Swirl System", *ASME paper GT2005-68939*. (2005)
- [9] Nunner, W., "Heat Transfer and Pressure Drop in Rough Vol. 202, 67-76. Tubes," *A.E.R.E. Library Translation 786* (1956).
- [10] E N Sieder & G E Tate, *Ind. Engineering Chemistry, Volume 28, Page 1429*, (1936).
- [11] Sun, Z., Chew, J., Hills, N., Volkov, K. and Barnes, C., "Efficient FEA/CFD Thermal Coupling For Engineering Applications", *Trans. ASME, Journal of Turbomachinery (to appear soon)*, see also *ASME paper GT2008-50638*. (2009)
- [12] Verdicchio, J.A., Chew, J.W., and Hills, N.J., "Coupled Fluid/Solid Heat Transfer computation of Turbine Discs", *ASME paper 2001-GT-0123*. (2001)